Modelling and Characterisation of Silicon Waveguides in Photonic Integrated Circuits

M. Ljubotina, M. Topič, J. Krč
University of Ljubljana, Faculty of Electrical Engineering, Tržaška cesta 25, 1000 Ljubljana, Slovenia
milos.ljubotina@fe.uni-lj.si

***Abstract*—Modelling and characterization of basic waveguiding structures in integrated photonics is important due to the large variety of established and emerging technologies used for fabrication. In this contribution we present a modelling and characterization approach for integrated silicon waveguides. We provide waveguide characteristics calculated from eigenmode simulation and optical measurement results.**

I. Introduction

The field of integrated photonics pertains to the integration of, otherwise discrete, optical and photonic components and devices. Photonic integrated circuits (PICs) are thus the photonic equivalent of electronic integrated circuits. Photonic integration is used in optical communications, sensing, imaging, signal processing, neuromorphic computing, quantum technologies, and other areas. Presently, silicon-based materials are among popular materials used for fabrication of PICs. This is largely due to their compatibility with the widespread complementary metal-oxide-semiconductor (CMOS) technology, thus leveraging decades of prior research and development in electronics. However, silicon-based materials do not present an all-purpose platform for photonic integration. Besides other established technologies, such as lithium niobate or III-V material platforms, new and emerging materials are pursued as well. Due to the variety of technologies used for photonic integration, modelling and characterisation of basic structures is an important topic.

In our conference presentation we will present the methods and results of optical modelling and characterisation of integrated optical waveguides based on the silicon-on-insulator (SOI) technology. Typical cross sections of rectangular (strip) SOI waveguides are 220 nm in height and around 500 nm in width, such that they assure single-mode operation with near-infrared light (e.g., wavelength of 1550 nm), as commonly used in optical communications. The optical behaviour of a waveguide is described by its effective refractive index and light transmission properties. These can be determined from known material properties through numerical simulation and experimentally from transmission measurements of different integrated structures, such as spirals, Mach-Zehnder interferometers (MZIs) [1], and ring resonators (RRs) [2]. The models associated with the considered structures and the waveguide properties will be introduced. Simulation will be used at the device and circuit level to determine the nominal waveguide properties and transmission spectra of the designed devices. Furthermore, corner analysis will be performed in consideration of fabrication variations of waveguide cross sections. Finally, the presented models will be used to extract the investigated waveguide properties from measured transmission spectra of physical devices.

II. Modelling

A. Waveguides

Waveguides are used to route light from one integrated component to another. Their two most important characteristics are their incurred optical losses and phase accumulation. Uniform sections of a waveguide can be described by Eq. 1:

$$\vec{E}(x,y,z,t) = \vec{E}(x,y)e^{-\left(\frac{\alpha}{2}+i\beta\right)z}e^{-i\omega t} \tag{1}$$

where $\vec{E}$ is the electric field, α is the power attenuation coefficient, $\beta = 2\pi n_{\mathrm{eff}}\lambda^{-1}$ is the phase constant, z is the direction of propagation, ω is the angular frequency, n_{eff} is the effective refractive index of the structure, and λ is the vacuum wavelength. However, waveguides often include bends, incurring additional optical loss due to changed waveguide properties and mode mismatch at straight-bend interfaces.

In our work, we model waveguides, focusing mainly on three characteristic parameters: n_{eff}, α_{dB}, and T_{sb}, where α_{dB} is the attenuation coefficient in decibels, and T_{sb} is the straight-bend interface power transmission ratio. To account for the wavelength dependence of the effective refractive index n_{eff}, a second degree polynomial is used around a central wavelength, as indicated in Eq. 2:

$$\begin{aligned} n_{\mathrm{eff}}(\lambda) &= n_{\mathrm{eff}}(\lambda_{\mathrm{c}}) + \left.\frac{\mathrm{d}n_{\mathrm{eff}}}{\mathrm{d}\lambda}\right|_{\lambda=\lambda_{\mathrm{c}}}(\lambda-\lambda_{\mathrm{c}}) \\ &\quad + \frac{1}{2}\left.\frac{\mathrm{d}^2 n_{\mathrm{eff}}}{\mathrm{d}\lambda^2}\right|_{\lambda=\lambda_{\mathrm{c}}}(\lambda-\lambda_{\mathrm{c}})^2 \\ &= n_1 + n_2(\lambda-\lambda_{\mathrm{c}}) + n_3(\lambda-\lambda_{\mathrm{c}})^2, \end{aligned} \tag{2}$$

where λ_{c} is the central wavelength, and n_{i} are the polynomial coefficients. Equivalently, the group index, $n_{\mathrm{g}} = n_1 - \lambda_{\mathrm{c}} n_2$ and dispersion parameter, $D = -2\lambda_{\mathrm{c}} c^{-1} n_3$, can be used instead of n_2 and n_3, where c is the speed of light in vacuum [1]. Similarly, straight-bend transmission is modelled with a polynomial given in Eq. 3:

$$T_{\mathrm{sb}}(\lambda) = x_1 + x_2(\lambda-\lambda_{\mathrm{c}}) + x_3(\lambda-\lambda_{\mathrm{c}})^2, \tag{3}$$

where x_{i} are polynomial coefficients. As the attenuation parameter α_{dB} is highly dependent upon the fabrication process, it is not determined from simulation.

B. Other devices

In addition to regular waveguides, devices considered in our work are spirals, Mach-Zehnder interferometers, and ring resonators. Spirals are modelled by their length, number of straight-bend interfaces, and the underlying waveguide properties, as shown in Eq. 4:

$$T = T_{\mathrm{sb}}^{N_{\mathrm{sb}}} 10^{-L\frac{\alpha_{\mathrm{dB}}}{10}}, \tag{4}$$

where T is the device power transmission, N_{sb} is the number of straight-bend interfaces, and L is the spiral length. The transmission of Mach-Zehnder interferometers is modelled with Eq. 5:

$$T = \frac{1}{4}e^{-\alpha L_0}\left[1 + 2e^{-\frac{\alpha}{2}\Delta L}\cos(\beta\Delta L) + e^{-\alpha\Delta L}\right], \tag{5}$$

978-1-6654-7899-1/22/$31.00 ©2022 IEEE

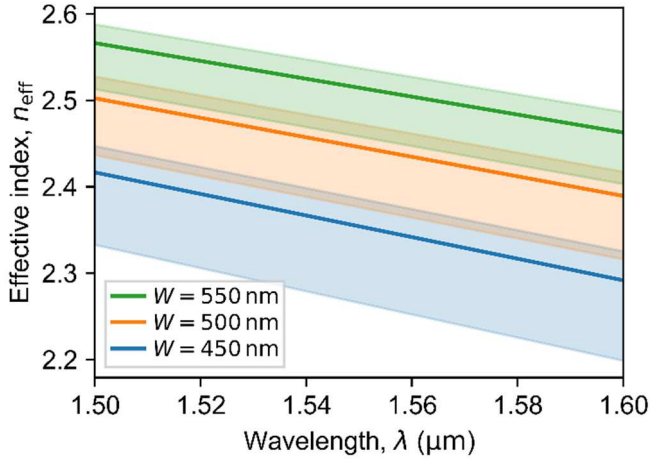

Fig 1: Effective refractive indices for three SOI waveguide widths (W) as obtained from waveguide simulations.

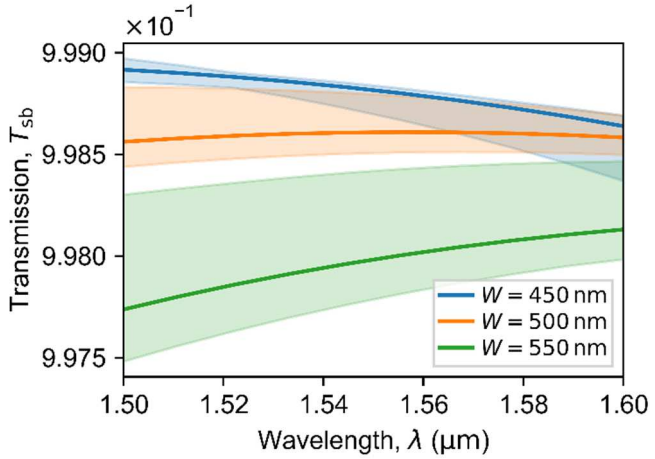

Fig 2: Straight-bend interface transmission for three SOI waveguide widths as obtained from waveguide simulations.

TABLE I
SIMULATED AND MEASURED WAVEGUIDE PARAMETERS

Calculated from	simulations	measurements
n_1	2.445919	2.447112
n_g	4.196590	4.189485
D (ps nm^{-1} km^{-1})	431.054	584.403
α_{dB} (dB cm^{-1})	7.000 [a]	6.101
T_{sb} (dB)	0.998608	0.998699

[a]Obtained from process development kit, not simulation [3].

where L_0 is the length of the shorter arm of the MZI, and ΔL is the difference between the lengths of both arms. Finally, the transmission spectrum of ring resonators is given by Eq. 6:

$$T = \frac{t^2 - 2ta\cos(\beta P) + a^2}{1 - 2ta\cos(\beta P) + (ta)^2}, \quad (6)$$

where t is the straight-coupling coefficient of the RR coupling section, a is the cavity round trip transmission, and P is the cavity perimeter.

III. RESULTS

Three different strip waveguide cross sections are considered. Their dimensions are 220 nm in height and 450 nm, 500 nm, and 550 nm in width. Fig. 1 shows the effective refractive indices of these waveguides obtained from eigenmode simulation, where W is the waveguide width, and the shaded regions represent ranges of possible values based on the corner analysis. The effective indices are larger for wider waveguides and decrease with increasing wavelength. Wavelength dependence appears linear; however, detailed analysis shows a slightly nonlinear relation, which can have an impact on the performance of integrated devices. The fabrication variation of the effective index decreases with increasing waveguide width.

For straight-bend interface transmission, bends with a constant bend radius of 5 μm are considered. Fig. 2 shows the simulated straight-bend interface transmission. The relation between T_{sb}, wavelength, and waveguide width is more complex than in the case of the effective index. Most of the considered wavelength range, narrower waveguides exhibit larger and more fabrication tolerant T_{sb}. Additionally, wavelength dependence of T_{sb} is clearly nonlinear.

Table I gives example end results of simulation and measurement for the 500 nm wide waveguide and central wavelength of 1550 nm. The refractive index parameters are in good agreement between measurement and simulation, with only the dispersion parameter exhibiting larger relative error. The value for the attenuation coefficient in the simulation segment of the table is taken from the utilised process development kit (PDK) [3]. The measured coefficient is similar to this value. Due to difficulties with the experimental part of our work, only a single parameter is shown for T_{sb} in this table. This parameter is in good agreement between simulation and measurement; however, further work is required to validate this result. The measured attenuation parameters are based on a further improved MZI model that accounts for Y-branch insertion loss and bends in the MZI arms [4].

In our presentation we will provide more detailed results for all model parameters and waveguide cross sections, including simulation and experiment results, as well as key considerations for further research.

IV. CONCLUSION

We have presented our modelling approach for waveguides and other integrated devices (spirals, MZIs, RRs), as well as selected simulation and experiment results for the effective refractive index and straight-bend interface transmission of three SOI waveguides. These results show good agreement between simulation and measurement. Further results and conclusions will be given in the presentation.

ACKNOWLEDGMENT

We acknowledge the financial support from the Slovenian Research Agency—ARRS (program P2-0415 and PhD funding for M.L.). We also acknowledge the team of the edX UBCx Phot1x Silicon Photonics Design, Fabrication and Data Analysis course 2021 organised by the University of British Columbia, Canada, for their support in design, fabrication, and characterisation of integrated photonic structures on SOI.

REFERENCES

[1] L. Chrostowski and M. Hochberg, *Silicon Photonics Design: From Devices to Systems*. Cambridge: Cambridge University Press, 2015. doi: 10.1017/CBO9781316084168.

[2] W. Bogaerts *et al.*, "Silicon microring resonators," *Laser & Photonics Reviews*, vol. 6, no. 1, pp. 47–73, 2012, doi: 10.1002/lpor.201100017.

[3] *SiEPIC_EBeam_PDK*. SiEPIC, 2022. Accessed: May 30, 2022. [Online]. Available: https://github.com/SiEPIC/SiEPIC_EBeam_PDK

[4] Y. Zhang *et al.*, "A compact and low loss Y-junction for submicron silicon waveguide," *Opt. Express, OE*, vol. 21, no. 1, pp. 1310–1316, Jan. 2013, doi: 10.1364/OE.21.001310